

# Amenability of Reduced Iron Ore Pellets to Mechanical Degradation

Fernando Oliveira BOECHAT,<sup>1)\*</sup> Leonardo Tomas da ROCHA,<sup>1,2)</sup> Rodrigo Magalhães de CARVALHO,<sup>1)</sup> Sung-Mo JUNG<sup>2)</sup> and Luís Marcelo TAVARES<sup>1)</sup>

1) Department of Metallurgical and Materials Engineering, COPPE, Universidade Federal do Rio de Janeiro, UFRJ, Rio de Janeiro, Brazil. 2) Environmental Metallurgy Laboratory, Graduate Institute of Ferrous Technology Pohang University of Science and Technology (POSTECH), Pohang, South Korea.

(Received on December 19, 2017; accepted on February 7, 2018; J-STAGE Advance published date: April 28, 2018)

The mechanical properties of iron ore pellets are of central importance to guarantee good productivity in direct reduction plants. Besides the generation of fines during handling, mechanical degradation resulting from forces produced inside the furnace are detrimental to the performance of these reactors, since they can lead to the generation of clusters, and also because they impact negatively the permeability of the charge to the flow of reducing gases. The present work analyzed the effect of different degrees of reduction on the mechanical properties of direct reduction iron ore pellets so as to estimate the proportion of fines generated inside a direct reduction furnace. As such, tests have been performed with unreduced, as well as iron ore pellets that were subjected to different degrees of reduction, with the aim of analyzing their mechanical properties, including microhardness, cold compression strength, mass loss in drop tests as well as pore size distributions. From these results, a parameter of a model of mass loss due to surface breakage was estimated, which demonstrated their greater amenability to breakage as reduction progressed. A combination of these results to simulations using the Discrete Element Method of a direct reduction furnace made it possible to estimate in 5.7% the percentage of fines generated in the furnace.

KEY WORDS: iron ore pellets; degradation; reduction.

## 1. Introduction

Iron ore pellets have characteristics that make them the preferred charge for direct reduction furnaces. Their uniformity in both size and chemical composition makes them particularly attractive for sponge iron producers. Another important characteristic of these agglomerates is their higher mechanical strength when compared to lump ore and sinter feed. In spite of that, iron ore pellets can still undergo degradation during handling from the induration furnace to the reduction furnace.

Breakage of pellets, such as other steelmaking materials, can occur as either surface or body breakage.<sup>1)</sup> Whatever fines are generated during handling from the induration furnace of the pelletizing plant to the reduction furnace of the steel mill, which can be located in different continents, can be removed by screening. However, fines that are generated inside the direct reduction furnace are particularly detrimental, since they will have a negative impact in the process, by promoting the generation of clusters and by reducing the permeability of the charge,<sup>2–4)</sup> which negatively impact productivity and metallization of the charge. It is estimated that the amount of fines that are either dragged by the reducing gases or that appear in the discharge of direct

reduction furnaces represents around 3 to 5.5% of the feed,<sup>5)</sup> not including those fines that are incorporated in clusters or sintered to other pellet particles.

One common method of assessing in the laboratory the proportion of fines that would be generated inside a reduction furnace is the reduction disintegration index (RDI) test. In this test the charge is subjected to reduction with a constant composition of the reducing gases at constant temperature. The reduced material is then weighed and subjected to sieving with opening of 3.15 mm. The percentage passing in this sieve is the value of RDI. Several researchers have studied degradation of iron ores under reduction at different temperatures and using different reducing gas composition using this test.<sup>6–11)</sup> That test, however, does not account for differences in stressing conditions that the pellet will encounter inside different reduction furnaces.

Huang *et al.*<sup>12)</sup> described the degradation mechanism of iron ore pellets that results from weakening of the microscopic structure during reduction. In this study the authors analyzed the hardness and cold crushing strength of pellets under different levels of reduction. That study demonstrated that a sharp drop in both crushing strength and hardness occurs at reductions as low as 10%. It also showed that at higher levels of reduction (>25%) a small increase in both occurred. Data from that work and additional work in the author's laboratory<sup>13)</sup> served as the basis for a recent

\* Corresponding author: E-mail: fboechat@globo.com  
DOI: <http://dx.doi.org/10.2355/isijinternational.ISIJINT-2017-734>

study,<sup>14)</sup> where the generation of fines in a direct reduction furnace was simulated by a combination of discrete element simulations and breakage modeling.

The present work studied the effect of reduction on the mechanical properties of an iron ore pellet, applying the findings to improving the prediction of degradation inside a direct reduction furnace.

**2. Material and Methods**

**2.1. Sample Preparation and Reduction**

A sample of an iron ore pellet produced in a pelletizing plant in Brazil served as the basis of the present work. Sieving demonstrated that 95% of the pellets (in weight) was contained in the range from 8 to 16 mm, and the 12.5–9.0 mm size range contained the largest proportion in pellets in weight, being therefore used as the basis of this work.

The as-received pellet sample presented the chemical composition given in **Table 1**. The ratio SiO<sub>2</sub>/CaO shown in the table, called binary basicity and equal to 0.9, is marginally higher than the value for typical direct reduction pellets, but still within market specifications. Iron in the pellets is predominantly present as hematite.

Samples were subjected to reduction at the temperature of 950°C in controlled atmosphere (**Table 2**) in a horizontal furnace (Lenton 17/300), which made it possible to insert a glass crucible that was capable of holding about 40 pellets each time. Gas flowrate was set to 1.055 l/min, which was selected on the basis of the two earlier studies.<sup>12,15)</sup> Screening experiments were conducted with batches of pellets that were subjected to reduction time intervals that ranged from 5 to 40 minutes in order to establish the relationship between time and degree of reduction. This degree of reduction was estimated using the expression

$$\text{Degree of reduction} = 100 \frac{\text{pellet mass before reduction} - \text{pellet mass after reduction}}{\text{pellet mass before reduction}} \dots\dots\dots (1)$$

From these preliminary results the durations of 5, 8 and 15 minutes were selected to allow reaching 5, 15 and 30% of reduction of the iron ore pellets, respectively. Upon completion of each test, samples were placed in inert atmosphere prior to further testing.

**2.2. Sample Testing**

With the aim of analyzing the mechanical response of the iron ore pellets during reduction, hardness measurements were conducted in a microhardness tester (HM220,

Shimadzu) with a load of 1 000 mN. The pellets, separated in different degrees of reduction, were placed in resin and their hardness measured in two different regions: the core and the surface. This later corresponded to indents that were placed in the outer 2 mm region of the pellets.

Cold compression crushing tests were carried out in an Instron MicroTester, at a loading rate of 10 mm/min, following the ISO4700 standard. Deformations, besides loads, were recorded during the tests, thus allowing to estimate the work required for pellet breakage. The data was then analyzed using order statistics.

With the aim of analyzing the generation of fines, self-breakage tests were carried out. These consisted of dropping pellets, one by one, from a height of one meter, onto a metal plate, weighing individual pellets after each impact in an analytic scale, up to a total of 10 impacts. At least 10 pellets were dropped for each level of reduction. The mass loss is given by

$$\text{Mass loss in nth impact} = 100 \frac{\text{pellet mass before nth impact} - \text{pellet mass after nth impact}}{\text{pellet mass before nth impact}} \dots\dots\dots (2)$$

Sample analyzes also included scanning their internal structure in an X-ray microtomograph (Skyscan 1 173 from Bruker), with 8 W power with a resolution of 18 microns per pixel. A total of five pellets were subjected to scanning under each reduction level.

**3. Results and Discussion**

**3.1. Relationship between Pore Size and Degree of Reduction**

A comparison is shown in **Fig. 1** of pellets with different degrees of reduction that were subjected to X-ray microtomography. As already observed by Huang *et al.*,<sup>12)</sup> porosity increased with the degree of reduction, thus leading to an increase in the number of defects in the pellet. The presence of cracks is evident in **Fig. 1(c)**, which will have a significant effect on pellets strength.

X-ray microtomography allowed measuring the pore size distribution, and **Fig. 2** analyzes the relationship between the mean pore size detected and the degree of reduction. It is evident that a measurable increase in pore size results from the first levels of reduction, reaching saturation at 15% of reduction. It may be inferred that such increase in porosity is responsible for the appearance of the cracks observed in **Fig. 1**. It is important to recognize that the X-ray tomograph used presented a resolution of 18 μm, which limited its ability to detect pores below this size.

**3.2. Relationship between Cold Compression Strength and Degree of Reduction**

Cold compression strength results are summarized in **Fig. 3**, demonstrating that reduction resulted in a significant drop in the strength of iron ore pellets. Indeed, significant reduction was found even after the lowest level of reduction studied (5%). In addition to that, there is some evidence that reduction also increased variability in the data in comparison to the unreduced pellets.

Results are also presented in summary in **Fig. 4**, which demonstrates the significant drop in strength from an aver-

**Table 1.** Chemical composition of the as-received pellets.

	Fe Total	SiO <sub>2</sub>	Al <sub>2</sub> O <sub>3</sub>	CaO	MgO	P	SiO <sub>2</sub> /CaO
mass concentration	67.0	1.7	0.5	1.6	0.15	0.05	0.90

**Table 2.** Composition of the reducing gas.

	H <sub>2</sub>	CO	CO <sub>2</sub>	Air
concentration	32.5	32.5	7.5	27.5

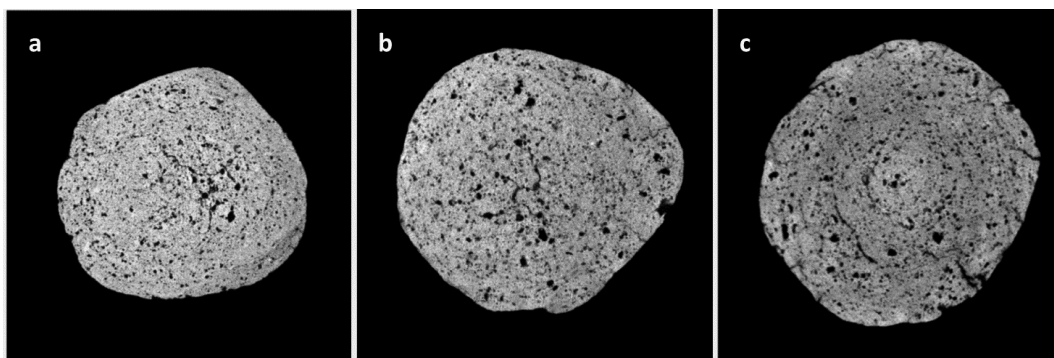


Fig. 1. X-ray microtomographic images of iron ore pellets after different degrees of reduction: 5% (a), 15% (b) and 30% (c).

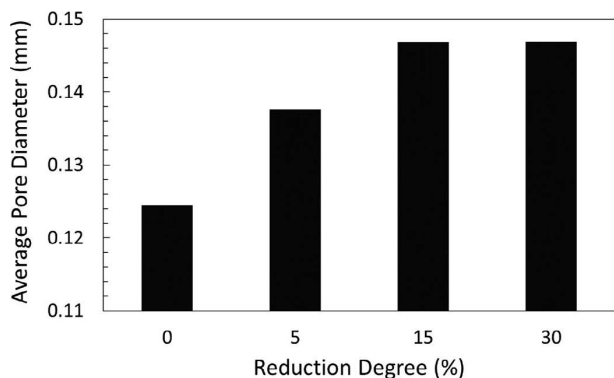


Fig. 2. Mean spherical equivalent pore size measured by X-ray microtomography.

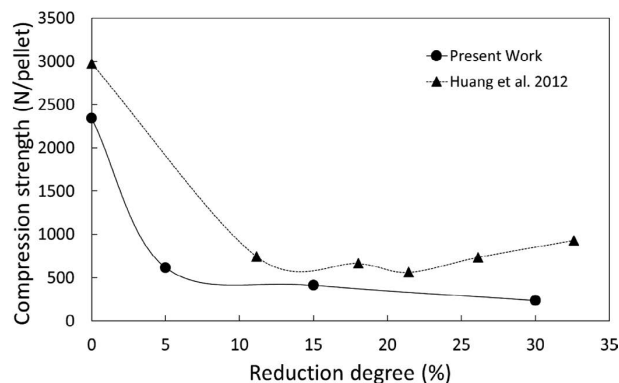


Fig. 4. Effect of degree of reduction on mean cold compressive strength of pellets, with comparison to data from Huang *et al.*<sup>12)</sup>

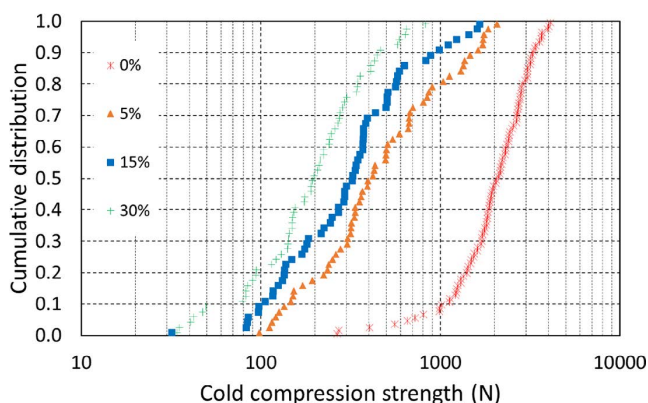


Fig. 3. Distribution of rupture force of 12.5–9.0 mm pellets as a function of degree of reduction. (Online version in color.)

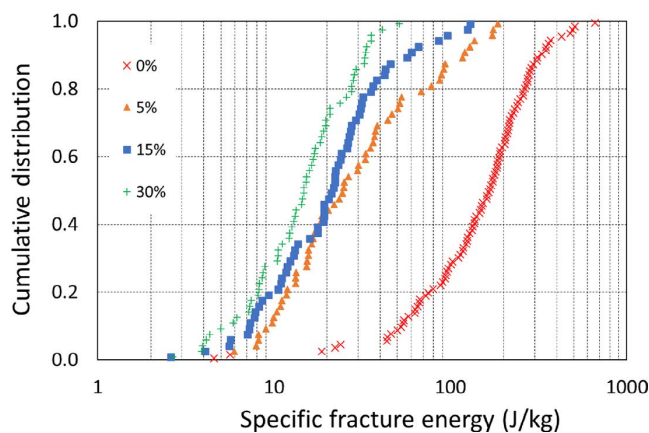


Fig. 5. Distribution of specific fracture energies of unreduced and reduced iron ore pellets. (Online version in color.)

age value of 2 344 N/pellet to about 617 N/pellet (73%) at the first level of reduction studied. These results are compared to those obtained by Huang *et al.*,<sup>12)</sup> which shows good general agreement. However, in the present work a monotonic reduction in strength was observed for higher levels of reduction, which contrasts with results from Huang *et al.*,<sup>12)</sup> which showed a modest recovery in strength at the highest levels of reduction studied, which the authors attributed to the healing of pores and cracks with wustite reduced to metallic iron. However, a question arises on the statistical significance of that gain in strength.

From the individual force-deformation profiles and the weights of each pellet it is possible to estimate the energy required for breaking each individual pellet. In Fig. 5 it is evident that a severe reduction occurs in the energy required to cause fracture of the pellets with even the lowest level of

reduction. The average fracture energy of pellets contained in the 12.5–9.0 mm size range reduced from 170 to 43 J/kg after only 5% reduction, which is a 76% drop. It shows that the change in internal structure brought by reduction of hematite to magnetite is the key responsible for the observed reduction in strength, a result that has also been observed by Huang *et al.*<sup>12)</sup> As pellets continue to undergo reduction the mean energy required to fracture pellets continues to drop, although not as significantly, reaching a mean value of only 17 J/kg after 30% reduction.

### 3.3. Relationship between Microhardness and Degree of Reduction

A summary of the mean values of microhardness of the

different regions of the pellet as a function of degree of reduction is presented in Fig. 6, which shows the severe drop in microhardness at the lowest level of reduction studied. This behavior is similar to the one already found in the case of specific fracture energies. Analyzing now the variation of microhardness at the different regions of the pellet it also becomes evident, as already observed by Huang *et al.*,<sup>12)</sup> that the hardness of the core continuously drops with increasing levels of reduction. However, in the case of the periphery, the value corresponding to 5% of reduction shows a significant drop, but then followed by a recovery in hardness at higher degrees of reduction. This may be explained by the fact that reduction occurs more rapidly (topochemical reaction) in the periphery of the pellets, with a quicker transformation of hematite to magnetite, which is associated to an increase in volume of about 24%.<sup>16)</sup> At higher levels of reduction, however, some metallic iron is also generated, which is responsible for some recovery of strength in this region, thus increasing locally the hardness. These findings are consistent with observations by other authors.<sup>12,16)</sup>

The additional drop in hardness when the degree of reduction increased from 15 to 30% may be due to transformation of magnetite to wüstite, which has been associated to an expansion in the internal volume<sup>16)</sup> of about 31% when compared to hematite.

### 3.4. Relationship between Mass Loss due to Surface Breakage and Degree of Reduction

The incremental mass loss of pellets owing to the low energy impacts (9.8 J/kg) is now analyzed. Figure 7 presents all data for the total number of impacts. It shows that a relatively modest increase in amenability to surface breakage occurs at only 5% of reduction. At increasing levels of reduction, however, the amenability to surface breakage increases significantly, reaching the highest level at 30% of reduction.

A summary of the results is presented in Fig. 8, which shows the variation of the mean mass loss due to surface breakage as a function of degree of reduction. It is evident that the average mass loss increases with the degree of reduction. These results contrast with the severe reduction in both microhardness and pellet strength observed previously for the lowest level of reduction studied.

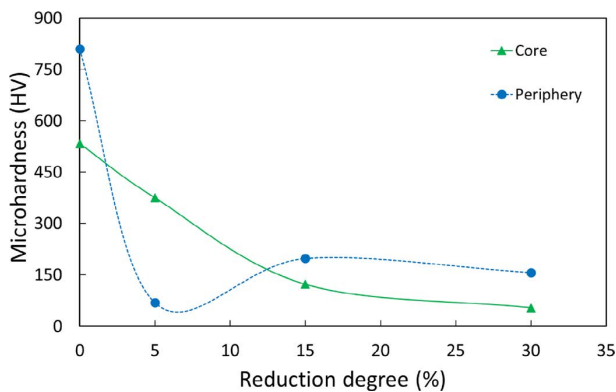


Fig. 6. Variation of microhardness of iron ore pellets as a function of degree of reduction and location in the pellet. (Online version in color.)

Boechat *et al.*<sup>14)</sup> demonstrated that a model could be used to describe the relationship between the effective collision energy  $E$  experienced by a pellet and the mass loss in every collision event by an unreduced pellet. It is given by

$$\text{Average mass loss} = k = a \left( \frac{E}{E_o} \right)^\lambda \dots\dots\dots (3)$$

where  $a$  and  $\lambda$  are dimensionless parameters that must be fit from data and  $E_o$  is a reference collision energy, taken as 10 J/kg.  $E$  is the effective mass-specific energy in each collision, obtained from a combination of the normal component of the energy dissipated in the normal direction of the collision added to 57% of the contribution from the shear or tangential component. In the case of the unreduced pellets analyzed in the present work it was found that the parameters  $a$  and  $\lambda$  were equal to 0.0012 and 1.24, respectively. If it is now assumed that the value of the exponent in Eq. (3) (parameter  $\lambda$ ) does not vary with degree of reduction – an assumption that is reasonable but that cannot be demonstrated to be valid at this time – then the values of the parameter  $a$  can be estimated for the different levels of reduction. This is illustrated in Fig. 9.

Cavalcanti<sup>13)</sup> demonstrated that the parameter  $a$  varies inversely with microhardness in unreduced pellets. The relationship between the parameter  $a$  in Eq. (3) and the microhardness in the case of the pellets in the present work is illustrated in Fig. 10. It shows that a significant drop in

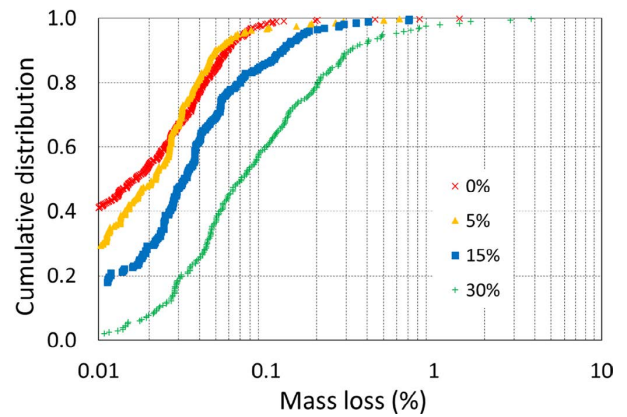


Fig. 7. Distribution of mass loss due to surface breakage from drops at 9.8 J/kg as a function of degree of reduction. (Online version in color.)

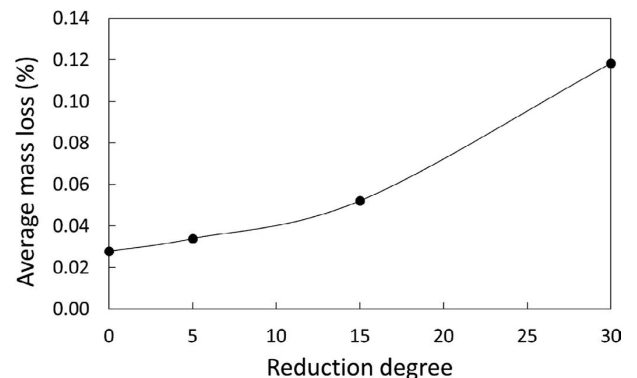
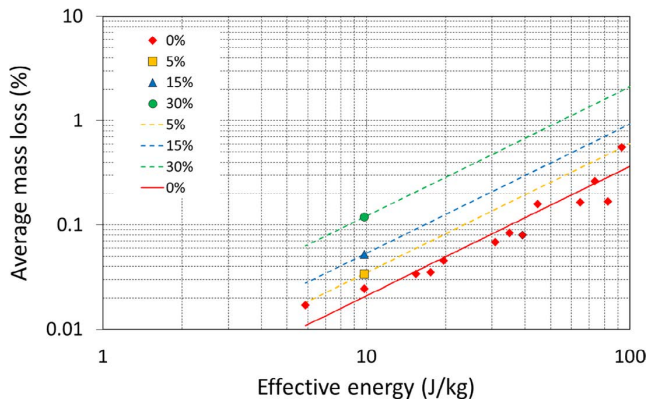
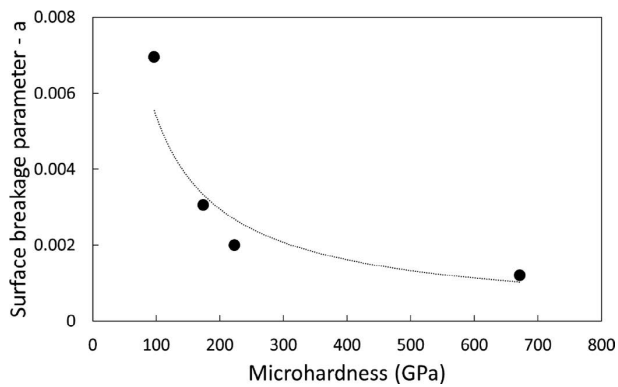


Fig. 8. Variation of surface mass loss per 9.8 J/kg impact as a function of degree of reduction.



**Fig. 9.** Average mass loss as a function of effective collision energy and degree of reduction, and comparison to data for unreduced pellet.<sup>13)</sup> Lines represent Eq. (3). (Online version in color.)



**Fig. 10.** Relationship between parameter  $a$  from Eq. (3) and average Vickers microhardness of reduced and unreduced pellets.

Vickers hardness is now accompanied by an equivalent increase in amenability to surface breakage for the lower degrees of reduction.

### 3.5. Generation of Fines during Reduction in a Direct Reduction Furnace

Analysis of data from cold compression (Figs. 3 and 5) and surface breakage tests (Fig. 7) demonstrates that the amenability of either catastrophic (body) breakage or surface (abrasion) breakage of iron ore pellets increases with degree of reduction. This is particularly critical in the case of direct reduction furnaces, in which pellets remain in solid form throughout the process.

In a recent publication by the authors<sup>14)</sup> the motion of pellets in a Minimod<sup>®</sup> MIDREX direct reduction furnace has been simulated using the discrete element method (DEM). An illustration of the simulated furnace, showing the compressive forces in the collisions is given in Fig. 11. It is evident that the lower part of the reduction section is subjected to higher loads, which coincides with the region in which pellets are reaching their higher level of reduction and have lower compressive strength and higher amenability to lose mass by abrasion (surface) breakage.

In these simulations the collision energy spectra have been calculated, which yielded the data depicted in Fig. 12 for different fractional depths in the reduction zone of the furnace. It is evident that the magnitude of collisions experienced by pellets increase with increasing the depth inside

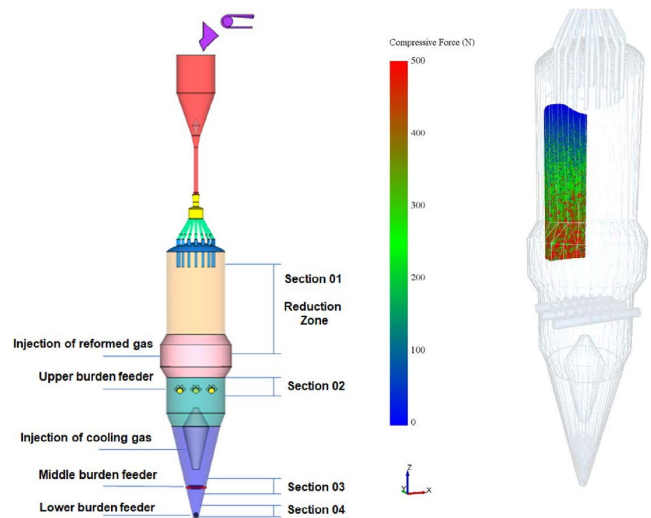


**Fig. 11.** Scheme of the direct reduction furnace (left) and result from simulation in the reduction zone, showing the profile of compression forces (right).<sup>14)</sup> (Online version in color.)

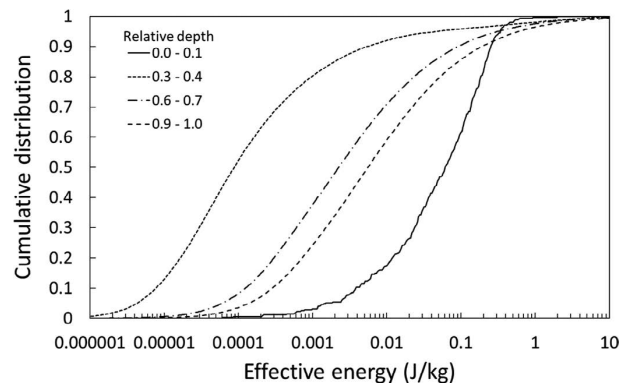


**Fig. 12.** Cumulative distribution of effective collision energy  $P(E)$  for different intervals of relative depth ( $h$ ) in the reduction zone of the direct reduction furnace.

the reduction zone of the furnace. Exception to this are the comparatively high magnitudes of collisions observed at very low relative depths, that is, close to the top of the reduction zone (Fig. 11), which are explained by the collisions of pellets from the feeding legs.

A first comparison of results from Figs. 12 and 5 shows that the proportion of collisions with magnitudes that would be sufficient to break (volume) pellets in the reduction zone of the furnace may be considered negligible. Such collisions, however, are likely to result in surface breakage of the pellets, which are described as follows.

In order to simulate surface breakage of pellets in the furnace, it is necessary to establish the relationship between the parameter  $a$  in the model (Eq. (3)) and the depth in the reduction zone inside the furnace. Using as a basis the model from Parisi and Laborde<sup>17)</sup> this relationship was proposed,<sup>14)</sup> being illustrated in Fig. 13. It is evident that a significant increase in parameter  $a$  occurs as the depth in the reduction zone increases, which contrasts with the results obtained by Boechat *et al.*<sup>14)</sup> on the basis of the work on unreduced pellets.<sup>13)</sup>

Assuming now that fragmentation occurs exclusively by surface breakage (abrasion) during the course of the pellet descent in the furnace, and assuming the validity of the assumptions listed by Boechat *et al.*,<sup>14)</sup> the generation of

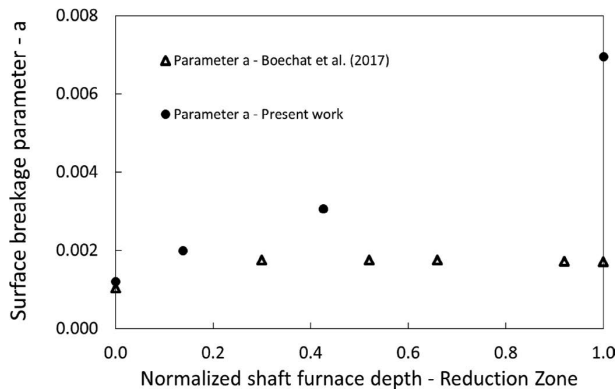


Fig. 13. Variation of surface breakage parameter a in Eq. (3) as a function of depth in the reduction section of the furnace.

Table 3. Percentage of fines predicted in the simulations for the different sections of the direct reduction furnace for the feedrate of 58 t/h.

Section in furnace	Boechat <i>et al.</i> (2018)	Present work
#01 – Reduction zone	3.42	5.59
#02 – Upper Burdenfeeder	0.07	0.04
#03 – Middle Burdenfeeder	0.01	0.02
#04 – Lower Burdenfeeder	0.03	0.07
Total	3.53	5.72

fines may be given by

$$w_{i,out} = w_{i,in} \int_0^1 \int_0^\infty p_i(E,h)[1 - k_i(E,h)] dEdh, \text{ for } i \neq n \dots (4)$$

$$w_{n,out} = 1 - \sum_{i=1}^{n-1} w_{i,out} \dots (5)$$

where  $w_i$  is the fraction of pellets contained in size  $i$ ,  $n$  is the number of size classes,  $p_i$  is the fraction of collisions involving material contained in size class  $i$ , and  $k_i$  is the proportion of debris from surface breakage resulting from collisions with magnitude  $E$  (effective specific energy) applied to each pellet and  $h$  is the fractional depth in the furnace, estimated using Eq. (3).

The proportion of material contained in the finest size range is given by

$$\text{Fines generated} = w_{n,out} - w_{n,in} \dots (6)$$

Equation (6) thus assumes that all fines generated by surface breakage have sizes below those of pellets fed to the furnace.

As such, the proportion of fines that would be expected at the discharge of the furnace may be predicted and a summary of the results is given in Table 3. These results are compared to those from Boechat *et al.*,<sup>14</sup> thus demonstrating that the data collected in the present work allowed updating the estimates, resulting in the proportion of fines generated as 5.7%, which is consistent with values observed inside industrial furnaces.<sup>5</sup>

#### 4. Conclusions

Experimental work involving reduced and unreduced iron

ore pellets allowed to conclude that:

- The average pore size increases with the degree of reduction;
  - A significant drop in hardness as well as in cold crushing strength of iron ore pellets occurs even after only 5% of reduction. However, unlike the findings of Huang *et al.*,<sup>12</sup> no increase in both hardness and cold crushing strength was observed at higher degrees of reduction;
  - Mass loss due to surface breakage (abrasion) increases four times as pellets were reduced, with this response increasing nearly proportionally to the degree of reduction;
- Simulations that combined experimental results from the present work with results from simulations using the discrete element method of a direct reduction furnace carried out in a previous work<sup>14</sup> allowed to conclude that:
- Some volume breakage of iron ore pellets is likely to occur in the furnace, with about 1.7% of the pellets broken;
  - Considering only surface breakage, it is predicted that the proportion of fines generated by surface breakage would be estimated in 5.7%, which is larger than the 3.5% reported in an earlier work by the authors, conducted without direct measurements on reduced pellets, but still consistent with reports from the literature. It demonstrates the importance of measuring directly, rather than inferring, the mechanical properties of pellets after reduction.

#### Acknowledgements

The authors would like to thank the financial support from the Brazilian research agency CNPq, as well as from Vale S.A. in the initial part of this investigation. The support of DEM Solutions for the use of the software EDEM under the Academic Program is also appreciated. Finally, the assistance from Laboratório de Instrumentação Nuclear from COPPE/UFRJ in the microtomography analysis was deeply appreciated.

#### REFERENCES

- 1) L. M. Tavares and R. M. Carvalho: *Int. J. Miner. Process.*, **101** (2011), 21.
- 2) A. Basdag and A. I. Arol: *Scand. J. Metall.*, **31** (2002), 229.
- 3) A. M. G. Bailon, H. O. Simões, P. G. Bueno, J. G. Pereira, T. M. Doellinger and M. R. R. Bianchi: Proc. 41st Seminar on Iron Ore and Raw Materials Reduction, ABM, Vila Velha, (2011), 1.
- 4) Y. W. Zhong, Z. Wang, X. Z. Gong and Z. C. Guo: *Ironmaking Steelmaking*, **39** (2012), 38.
- 5) Midrex Technologies: Direct from Madre - 3rd/4th Quarter 2011, <http://www.midrex.com/assets/user/media/DFM2011Q3-4.pdf>, (accessed 2017-08-11).
- 6) S. Dwarapudi and M. Ranjan: *ISIJ Int.*, **50** (2010), 1581.
- 7) T. Umadevi, P. Kumar, N. F. Lobo, M. Prabhu, P. C. Mahapatra and M. Ranjan: *ISIJ Int.*, **51** (2011), 14.
- 8) S.-L. Wu, X.-Q. Liu, Q. I. Zhou, J. Xu and C.-S. Liu: *J. Iron Steel Res. Int.*, **18** (2011), No. 8, 20.
- 9) T. Murakami, T. Kodaira and E. Kasai: *ISIJ Int.*, **55** (2015), 1181.
- 10) M. Mizutani, T. Nishimura, T. Orimoto, K. Higuchi, S. Nomura, K. Saito and E. Kasai: *ISIJ Int.*, **57** (2017), 1499.
- 11) L. Yi, Z. Huang, T. Jiang, R. Zhong and Z. Liang: *Powder Technol.*, **317** (2017), 89.
- 12) Z. Huang, L. Yi and T. Jiang: *Powder Technol.*, **221** (2012), 284.
- 13) P. P. S. Cavalcanti: M.Sc. thesis, Universidade Federal do Rio de Janeiro, (2015), <http://www.metalmat.ufrj.br/index.php/br/pesquisa/producao-academica/-/7/2015-2/286--265/file>, (accessed 2017-08-08) (in Portuguese).
- 14) F. O. Boechat, R. M. De Carvalho and L. M. Tavares: *Kona (Powder Part. J.)*, **35** (2018), doi: 10.14356/kona.2018009.
- 15) M. I. A. Barustan: M.Sc. thesis, GIFT, POSTECH, (2017).
- 16) J. Li: Ph.D. thesis, Central South University, (2007).
- 17) D. R. Parisi and M. A. Laborde: *Chem. Eng. J.*, **104** (2004), 35.